Neurobiology of Aging 35 (2014) 1491–1498

Contents lists available at ScienceDirect

Neurobiology of Aging

journal homepage: www.elsevier.com/locate/neuaging

Widespread RNA metabolism impairment in sporadic inclusion body myositis TDP43-proteinopathy☆

Andrea Cortese [a,g,1], Vincent Plagnol [f,1], Stefen Brady [a], Roberto Simone [b], Tammaryn Lashley [c], Abraham Acevedo-Arozena [h], Rohan de Silva [b], Linda Greensmith [a,d], Janice Holton [a,c], Michael G. Hanna [a], Elizabeth M.C. Fisher [a,e], Pietro Fratta [a,e,*]

[a] MRC Centre for Neuromuscular Disease, UCL Institute of Neurology, London, UK
[b] The Reta Lila Weston Institute, UCL Institute of Neurology, London, UK
[c] Department of Molecular Neuroscience, Queen Square Brain Bank, UCL Institute of Neurology, London, UK
[d] Sobell Department of Motor Neuroscience and Movement Disorders, UCL Institute of Neurology, London, UK
[e] Department of Neurodegenerative Disease, UCL Institute of Neurology, London, UK
[f] UCL Genetics Institute, University College London, London, UK
[g] Department of General Neurology, C. Mondino National Institute of Neurology Foundation, IRCCS, Italy
[h] Mammalian Genetics Unit, MRC, Oxfordshire, UK

ARTICLE INFO

Article history:
Received 21 August 2013
Received in revised form 14 December 2013
Accepted 25 December 2013
Available online 30 December 2013

Keywords:
TDP-43
Inclusion body myositis
RNA
MAPT
hnRNP
Amyotrophic lateral sclerosis

ABSTRACT

TDP43 protein mislocalization is a hallmark of the neurodegenerative diseases amyotrophic lateral sclerosis and frontotemporal dementia, and mutations in the gene encoding TDP43 cause both disorders, further highlighting its role in disease pathogenesis. TDP43 is a heterogenous ribonucleoprotein, therefore suggesting that alterations in RNA metabolism play a role in these disorders, although direct evidence in patients is lacking. Sporadic inclusion body myositis (sIBM) is the most common acquired myopathy occurring in adults aged older than 50 years and abnormal cytoplasmic accumulations of TDP43 have been consistently described in sIBM myofibers. Here, we exploit high quality RNA from frozen sIBM muscle biopsies for transcriptomic studies on TDP43-proteinopathy patient tissue. Surprisingly, we found widespread sIBM-specific changes in the RNA metabolism pathways themselves. Consistent with this finding, we describe novel RNA binding proteins to mislocalize in the cytoplasm of sIBM myofibers and splicing changes in MAPT, a gene previously shown to play a role in sIBM. Our data indicate widespread alterations of RNA metabolism are a novel aspect of disease pathogenesis in sIBM. These findings also document an association, in TDP43-proteinopathy patients, between heterogenous ribonucleoprotein pathology and RNA metabolism alterations and carry importance for neurodegenerative diseases, such as amyotrophic lateral sclerosis and frontotemporal dementia.

1. Introduction

TDP43 is a 414-amino acid, prevalently nuclear, RNA binding protein, encoded by the *TARDBP* gene, which is involved in numerous aspects of RNA metabolism including messenger RNA (mRNA) splicing, stabilization, transport, and micro RNA biogenesis (Cohen et al., 2011; Kawahara and Mieda-Sato, 2012). TDP43 is a major component of the inclusions that characterize frontotemporal dementia (FTD) and amyotrophic lateral sclerosis (ALS) central nervous system pathology, and sporadic inclusion body myositis (sIBM) muscle pathology (D'Agostino et al., 2011; Hernandez Lain et al., 2011; Küsters et al., 2009; Mackenzie et al., 2010; Olivé et al., 2009; Salajegheh et al., 2009; Weihl et al., 2008). As *TARDBP* mutations are also causative for both ALS and FTD, TDP43 may play a primary unknown pathogenic role in these disorders, now referred to as "TDP43 proteinopathies" (Kabashi et al., 2008; Mackenzie et al., 2010; Sreedharan et al., 2008). However, although impairment in

* Corresponding author at: Department of Neurodegenerative Disease, UCL Institute of Neurology, Queen Square, London, UK. Tel.: +44 (0)2034484448; fax: +44 207 837 8047.
E-mail address: pietro.fratta@gmail.com (P. Fratta).

[1] These authors contributed equally to this work.

0197-4580/$ – see front matter © 2014 The Authors. Published by Elsevier Inc. All rights reserved.
http://dx.doi.org/10.1016/j.neurobiolaging.2013.12.029

RNA metabolism through TDP43 gain or loss of function has been hypothesized (Lee et al., 2012; Polymenidou et al., 2011a; Tollervey et al., 2011a), the poor quality of endstage brain postmortem material means this yet remains to be demonstrated in patients.

sIBM is the most common muscle disease in adults aged older than 50 years. sIBM muscle pathology is characterized by three main components: (1) inflammatory changes; (2) degenerative features; and (3) mitochondrial alterations (Amato and Barohn, 2009; Engel and Askanas, 2006; Needham and Mastaglia, 2007). The pathogenesis of the disease is poorly understood and both inflammatory and degenerative mechanisms may play a primary role (Engel and Askanas, 2006; Needham and Mastaglia, 2007).

The numerous recent findings of cytoplasmic TDP43 inclusions in sIBM muscle fibers (D'Agostino et al., 2011; Hernandez Lain et al., 2011; Olivé et al., 2009; Salajegheh et al., 2009; Weihl et al., 2008), have strengthened the link between sIBM and neurodegenerative disorders, also supported by: (1) age of disease onset and its unresponsiveness to immunosuppressive treatment; (2) identification of numerous neurodegeneration-characteristic proteins in the ubiquitinated inclusions of sIBM muscle, such as abeta and tau (Supplementary Table 2) (Askanas et al., 2009; Mirabella et al., 1996); and (3) identification of mutations in the *VCP* gene as a cause of both ALS, and a complex phenotype which comprises an hereditary form of inclusion body myopathy associated with FTD (Johnson et al., 2010; Nalbandian et al., 2011).

Here, we exploit the excellent preservation of sIBM frozen muscle biopsies to conduct pathology and transcriptomic analysis on serial sections of patient TDP43-proteinopathy tissue. Surprisingly, we find widespread disruption in RNA metabolism and for the first time, we believe, document such changes in patient TDP43-proteinopathy tissue.

2. Methods

2.1. Patients

Muscle biopsies were obtained from 6 sIBM patients and 3 polymyositis (PM) patients. Muscle biopsies from 4 patients investigated for cramps or fatigue with normal examination and neurophysiology tests and normal histology were used as control subjects. In sIBM and PM patients, biopsies were all taken from moderately affected muscle and processed for routine histology and immunohistochemistry. If present, fibrosis and fatty muscle infiltration were never so widespread to hamper a definite pathologic diagnosis. sIBM patients fulfilled Griggs criteria for sIBM (Griggs et al., 1995). PM patients reported subacute proximal muscle weakness, had raised plasma creatine kinase levels, were steroid responsive and fulfilled Bohan and Peter criteria (Bohan and Peter, 1975). Biopsies were stored at −80 °C. Details of patients and pathologic findings are summarized in Supplementary Table 1. Institutional board reviewed the study and ethical approval was obtained.

2.2. RNA extraction

Twenty-five slides 20-μm thick of muscle biopsies of normal and patient muscle samples were homogenized in 1 mL of Trizol at 4 °C. RNA was isolated using RNeasy mini kit (Quiagen). RNA concentrations were determined using Nanodrop spectrophotometer (ND-1000). RNA was further analyzed for RNA quality on Agilent Bioanalyzer, which showed RNA integrity number >6 for all samples.

2.3. Array hybridization

Up to 2 mg of total RNA was processed and labeled using the Affymetrix GeneChip (Affymetrix, Santa Clara, CA, USA) whole transcript sense target labeling assay as outlined in the manufacturer's instructions. Hybridization to Affymetrix Human Exon 1.0 ST arrays was performed for 16 hours at 45 °C with constant rotation. The arrays were scanned with an Affymetrix Gene Chip scanner 3000-system (Affymetrix). Initial data were processed to CEL files using GeneChip operating software There are no versions to specify for this sofware (Affymetrix).

2.4. Analysis of array gene expression data

Graphical plots of unsupervised hierarchical clustering were generated using the Partek Genomic suite 6.6. All other statistical analyses related to the expression data, including differential expression analysis and principal component analysis (PCA) plots, were generated using the R statistical software (v2.15.0), in conjunction with the Bioconductor package limma (Smyth, 2004). Microarray expression data were normalized using the robust multi-array average procedure (Irizarry et al., 2003). For the differential expression analysis, genes were ranked based on a *t* test analysis and *p*-values were corrected for multiple testing using a Benjamini-Hochberg False Discovery Rate (FDR) correction (Benjamini and Hochberg, 1995).

Probe sets expression plots of genes of interest were subjected to visual inspection to identify candidate alternatively spliced exons. Lists of significantly up- and down-regulated genes obtained from statistical comparison were subjected to functional enrichment analysis using DAVID (Database for Annotation, Visualization and Integrated Discovery) (Huang et al., 2009). Exon array data are available under accession number E-MTAB-2141 at the ArrayExpress database (http://www.ebi.ac.uk/arrayexpress/).

2.5. Geneset enrichment analysis

GeneSet enrichment analysis was performed ranking datasets by signal-to-noise ratio. Permutations were carried out by geneset (n = 1000) (Subramanian et al., 2005) http://www.broadinstitute.org/gsea/index.jsp.

2.6. Reverse Transcriptase-Polymerase Chain Reaction (RT-PCR)

Total RNA (150 ng) was reverse transcribed into first-strand complementary DNA (cDNA) using SuperScript VILO cDNA Synthesis Kit (Invitrogen, Camarillo, CA, USA) and oligo(Dt). cDNA template was amplified using FastStart PCR Master mix (Roche (Roche Diagnostics Ltd., Basel, Switzerland)) in a TC-Plus Thermocycler (Techne, Burlington, NJ, USA). Primer sequences to amplify *MAPT* exons 2, 6, and 10 and reference genes are as following: GAPDH-F CCATGGCACCGTCAAGGCTGA; GAPDH-R GCCAGTAGAGGCAGGGAT GAT; 18S-F AAACGGCTACCACATCCAAG; 18S-R CGCTCCCAAGATCC AACTAC; MAPT-Ex9F AAGTCGCCGTCTTCCGCCAAG; MAPT-Ex11R GTCCAGGGACCCAATCTTCGA; MAPT-Ex4-6F GAAGACGAAGCTGCTG GTCA; MAPT-Ex4-6R TTGAGTTTCATCTCCTTTGC; MAPT-N-F CTTCTC CTCCTCCGCTGTC; MAPT-0N-R CTGCTTCTTCAGCTTTCAGG; MAPT-1N-R ATGCCTGCTTCTTCAGCTTC; MAPT-2N-R GAGCTCCCTCATCCACTAAGG.

PCR conditions were as follows: 5 minutes at 95 °C, and then 28–34 cycles of 30 seconds at 94 °C, 30 seconds at 59 °C, 1 minute at 72 °C with a final 10 minute extension at 72 °C. RT-PCR products were detected on 2% agarose gel: 4R and 3R tau RT-PCR products were 381 and 288 bp, respectively. The expected size for the PCR product bearing *MAPT* exon 6 is 278 bp, whereas the products for tau 0N, 1N, 2N, have an expected size of 212 bp, 303 bp, and 320 bp, respectively. The expected sizes of the PCR products for *GAPDH* and 18S were respectively, 469 bp and 250 bp.

To calculate exon inclusion *(I)*, the intensity of the peak representing exon inclusion was divided by the intensity of peaks

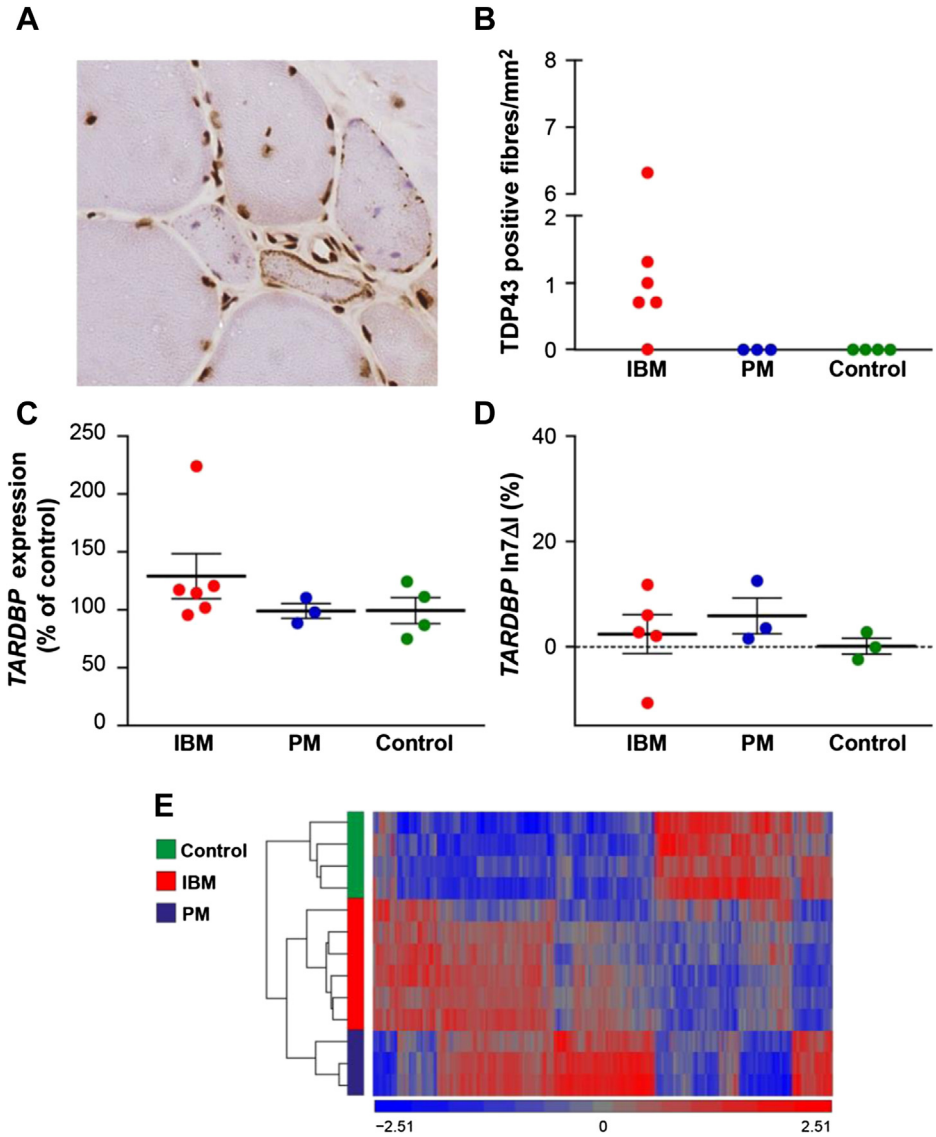

Fig. 1. Immunohistochemistry analysis and transcriptomics performed on serial muscle sections. (A) Immunohistochemistry shows abnormal TDP43 cytoplasmic localization and nuclear depletion (arrow) in sIBM myofibers. (B) Quantification of fibers with TDP43 mislocalization normalized to biopsy surface area. (C) *TARDBP* expression measured with Nanostring and (D) *TARDBP* 3′UTR intron 7 alternative splicing show (In7ΔI indicates % changes in TARDBP intron 7 inclusion rate vs. control) no significant changes amongst disease groups. (E) Exon array hierarchical clustering. IBM sample 4 is the sample with the highest presence of TDP43 inclusions (B), the highest *TARDBP* levels (C) and lowest rate of *TARDBP* intron 7 inclusion (D). Abbreviations: IBM, inclusion body myositis; PM, polymyositis; sIBM, sporadic inclusion body myositis.

representing both exon inclusion and exon skipping. Splicing change *(ΔI)* was calculated by subtracting exon inclusion in the sIBM or PM patients from the inclusion in control subjects (Tollervey et al., 2011a). Statistical methods used to compare *I* and *ΔI* of different exons across groups are outlined in Nanostring methods paragraph.

2.7. Nanostring

Validation of microarray data was carried out on 23 genes using NanoString nCounter (Seattle, WA, USA) on 11 of the 13 samples (5 sIBM, 3 PM, and 3 control subjects), excluding the 2 outliers IBM5 and Control3 as identified by microarrays. Probe hybridization was carried out with 500-ng RNA for 18 hours in an automated nCounter machine at NanoString. All genes on the nCounter CodeSet were analyzed simultaneously in true multiplex fashion. Three replicate runs were performed separately. Counts were collected as XLS files and then processed in 2 steps. Raw counts were first normalized using the mean of 6 internal spike-in positive control probes for all samples to account for systematic differences between assays. These control-normalized counts were then further normalized to the expression level of 6 reference genes (*ABCF1*, *ALAS1*, *LDHA*, *POLRI1B*, *RPLP0*, *SDHA*) that we selected as the most stable, with different expression levels, based on microarray results. For data presentation, each gene count value is shown as the mean of the replicates. To calculate exon inclusion same methods as described in RT-PCR section were applied. Statistical analysis of Nanostring and RT-PCR data were performed using Graphpad Prism 5 software (GraphPad Software Inc). Continuous variables were analyzed using either a 2-tailed *t* test or a Mann–Whitney U test as appropriate. If more than 2 groups were compared either analysis of variance or Kruskal-Wallis test was used. The statistical significance level was established at $p \leq 0.05$.

2.8. Immunohistochemistry

To compare the mRNA expression data with the protein expression of relevant genes, serial 7-μm frozen muscle sections of the 13 samples were processed for immunostaining. The following antibodies were used: TDP43 (Abnova, Taipei City, Taiwan; 1:800); heterogenous ribonucleoprotein (hnRNP) A2/B1 (Abcam, UK; 1:100); hnRNP C1/C2 (Abcam, UK; 1:200); hnRNP H (Abcam, UK; 1:200). Briefly, frozen sections were postfixed in 4% paraformaldehyde for 30-minutes at room temperature. Endogenous peroxidase activity was blocked with 0.3% H_20_2 in methanol and nonspecific binding with 10% dried milk solution. Tissue sections were incubated with the primary antibodies overnight at 4 °C followed by biotinylated anti-mouse IgG (1:200, 30 minutes; DAKO) (DAKO, Glostrup, Denmark) and ABC complex (30 minutes; DAKO) (DAKO, Glostrup, Denmark). Color was developed with di-aminobenzidine-H_20_2. Finally, counterstaining with hematoxylin was performed. The immunostained sections were imaged with Olympus BX41 (Melville, NY, USA).

3. Results and discussion

3.1. sIBM muscles show clear TDP43 pathology, but no changes in TARDBP *transcript level*

To obtain transcriptomic data from pathologically well-characterized tissue, we generated histology sections and RNA from serial muscle biopsy sections of patients with sIBM (n = 6), PM (n = 3), which presents inflammatory features similar to sIBM (Rayavarapu et al., 2011), and normal control subjects (n = 4) (clinical details—Supplementary Table 1). We obtained expression data using Affymetrix Exon 1.0 ST arrays, which target 270,366 human exons, and Nanostring nCounter gene expression, which allows direct detection of RNA molecules.

TDP43 immunohistochemistry (IHC) showed pathologic cytoplasmic staining in all but one sIBM patient (sIBM5) (Fig. 1). The aggregates appeared as punctate cytoplasmic staining or larger cytoplasmic inclusions. No TDP43 immunoreactivity was observed outside nuclei in PM and normal control subjects.

TARDBP mRNA expression levels are tightly autoregulated by a complex mechanism that acts through TDP43 binding its own transcript and regulating an alternative splicing event in the 3′UTR (Avendano-Vazquez et al., 2012), and have been reported to be increased or unchanged in TDP43-proteinopathies (Avendano-Vazquez et al., 2012; D'Agostino et al., 2011; Mishra et al., 2007; Olivé et al., 2009; Salajegheh et al., 2009; Weihl et al., 2008). We investigated upregulation and changes in the autoregulation pattern by microarray and targeted Nanostring analysis and found no evidence of differences in sIBM samples, although one sample (sIBM4), that had by far the most severe TDP43 pathology, had an increase in *TARDBP* mRNA and changes in the autoregulation pattern compatible with an attempt to compensate for high levels of TDP43 protein (Fig. 1). sIBM4 was also characterized by having the longest interval between onset and biopsy (Supplementary Table 1). These results suggest a subset of samples may show upregulation, which may explain the conflicting results in the literature, and future studies will be useful to assess if this phenomenon is related to the stage of disease.

Also, most of the transcripts which encoding proteins which are relevant to sIBM pathology accumulations, as comprehensively reviewed by Askanas et al., (2009), showed no significant evidence of increased mRNA levels (Supplementary Table 2).

Table 1
Gene ontology analysis of sIBM versus control DEGs and PM versus control DEGs show strong involvement of inflammatory pathways

Gene ontology category	Enriched gene ontology term		Number of listed genes in term	% of genes listed in term	Fold enrichment	FDR False discovery rate	Enriched gene ontology term		Number of listed genes in term	% of genes listed in term	Fold enrichment	FDR False discovery rate
	IBM						PM					
Biological process	GO:0006955	Immune response	200	6.2	1.7	2.51×10^{-11}	GO:0009611	Response to wounding	168	4.4	1.5	1.51×10^{-6}
	GO:0042110	T cell activation	50	1.5	2.3	1.85×10^{-5}	GO:0006955	Immune response	202	5.3	1.5	6.49×10^{-6}
	GO:0050867	Positive regulation of cell activation	43	1.3	2.2	5.06×10^{-4}	GO:0006954	Inflammatory response	109	2.9	1.6	7.18×10^{-5}
	GO:0042981	Regulation of apoptosis	189	5.8	1.3	3.93×10^{-2}	GO:0042110	T cell activation	47	1.2	1.8	2.95×10^{-2}
Cellular component	GO:0005886	Plasma membrane	845	26.1	1.2	3.33×10^{-13}	GO:0005886	Plasma membrane	1006	26.3	1.3	2.44×10^{-23}
	GO:0005887	Integral to plasma membrane	277	8.6	1.3	1.88×10^{-3}	GO:0005887	Integral to plasma membrane	371	9.7	1.5	3.52×10^{-16}
Molecular function	GO:0004984	Olfactory receptor activity	115	3.6	1.7	1.41×10^{-5}	GO:0015629	Actin cytoskeleton	88	2.3	1.6	5.08×10^{-3}
							GO:0003779	Actin binding	99	2.6	1.5	7.43×10^{-3}

Key: DEGs, differentially expressed genes; IBM, inclusion body myositis; PM, polymyositis; sIBM, sporadic inclusion body myositis.

A

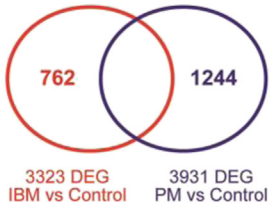

B

Gene Ontology Category	Enriched Gene Ontology Term		Number of listed genes in term	% of genes listed in term	Fold Enrichment	Benjamini	FDR
Cellular Component	GO:0005730	nucleolus	55	7.4	2.0	4.32E-04	1.43E-03
	GO:0030529	ribonucleoprotein complex	42	5.6	2.1	2.64E-03	1.75E-02
	GO:0031981	nuclear lumen	89	11.9	1.6	2.29E-03	2.28E-02
	GO:0070013	intracellular organelle lumen	101	13.5	1.4	1.07E-02	1.43E-01
	GO:0031974	membrane-enclosed lumen	103	13.8	1.4	1.73E-02	2.90E-01
	GO:0043233	organelle lumen	101	13.5	1.4	1.64E-02	3.29E-01
Kegg Pathway	hsa05016	Huntington's disease	18	2.4	3.4	2.99E-03	2.23E-02
	hsa03018	RNA degradation	9	1.2	5.3	1.95E-02	2.93E-01
	hsa05012	Parkinson's disease	13	1.7	3.5	1.76E-02	3.97E-01
	hsa00190	Oxidative phosphorylation	13	1.7	3.4	1.64E-02	4.93E-01
	hsa03010	Ribosome	10	1.3	3.9	3.23E-02	1.22E+00

C

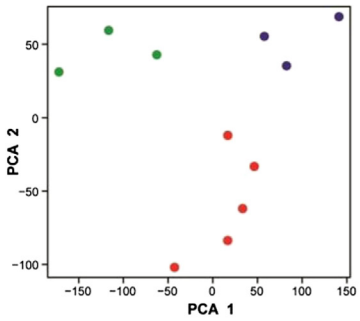

D

Gene Ontology Category	Enriched Gene Ontology Term		Number of listed genes in term	% of genes listed in term	Fold Enrichment	Benjamini	FDR
Biological Process	GO:0006414	translational elongation	14	7.6	14.8	7.70E-09	1.35E-08
	GO:0000377	RNA splicing, via transesterification reactions with bulged adenosine as nucleophile	10	5.4	7.0	3.79E-03	1.99E-02
	GO:0000398	nuclear mRNA splicing, via spliceosome	10	5.4	7.0	3.79E-03	1.99E-02
	GO:0000375	RNA splicing, via transesterification reactions	10	5.4	7.0	3.79E-03	1.99E-02
Cellular Component	GO:0031981	nuclear lumen	48	26.1	3.4	1.65E-12	1.02E-11
	GO:0030529	ribonucleoprotein complex	28	15.2	5.6	3.48E-11	4.30E-10
	GO:0005730	nucleolus	32	17.4	4.7	2.54E-11	4.70E-10
	GO:0070013	intracellular organelle lumen	49	26.6	2.8	2.00E-10	4.93E-09
Molecular Function	GO:0003723	RNA binding	36	19.6	5.0	4.03E-13	1.91E-12
	GO:0003735	structural constituent of ribosome	13	7.1	7.7	1.46E-05	1.39E-04

Fig. 2. sIBM specific gene ontology (GO) analysis highlights dysregulation of RNA-related pathways. (A) Representation of sIBM versus control and PM versus control DEGs. (B) GO analysis on sIBM specific DEGs highlights RNA related pathways and neurodegenerative diseases. (C) PCA1 and PCA2 analysis clusters samples by disease group; PCA1 separates controls from both sIBM and PM, although PCA2 differentiates sIBM samples from both control and PM cases. (D) GO performed on genes contributing to the PCA2, confirms the dominant presence of RNA metabolism pathways. Abbreviations: DEGs, differentially expressed genes; PM, polymyositis; sIBM, sporadic inclusion body myositis.

3.2. Identification of sIBM specific transcripts points to widespread alterations in RNA metabolism

Unsupervised hierarchical clustering of exon array data clearly separated samples according to the disease group (Fig. 1E). PCA, showed clustering of samples by disease group, but also identified 2 outliers: sIBM5, which was also atypical in lacking TDP43-aggregates, and control sample 12, which were therefore removed from further analysis (Supplementary Fig. 1). Exon arrays detected expression of >22,000 transcripts, and statistical analysis identified 3323 and 3931 differentially expressed genes (DEG) that passed the FDR-adjusted threshold (Benjamini-Hochberg FDR <0.05), between control subjects and sIBM and PM, respectively. Array data validation was carried out using the Nanostring platform to measure expression of 23 transcripts and by performing a comparison of DEGs using publicly available microarray expression data on sIBM muscle (Supplementary Tables 2a and 2b).

Gene ontology (GO) analysis for FDR-significant genes using DAVID (Database for Annotation, Visualization and Integrated Discovery) (Huang et al., 2009), not surprisingly showed enrichment of inflammatory-related terms, with GO terms being common to sIBM and PM compared with control subjects (Table 1).

To identify sIBM specific DEGs, which are not a consequence of the inflammatory process, we exploited the expression data from PM samples, which have a very similar inflammatory infiltrate to sIBM. We used 2 analytical approaches.

Firstly, using a 2-step procedure, we removed from the 3323 DEGs in sIBM versus control subjects, those also differentially expressed in PM versus control subjects (FDR < 0.05). This analysis identified 762 sIBM specific DEGs and 1244 PM specific DEGs (Fig. 2A). GO analysis for sIBM revealed enrichment of ribonucleoprotein complex and other ribonucleoprotein related terms (Fig. 2B). Significant enrichment for RNA degradation, oxidative phosphorylation, Parkinson disease, and Huntington disease KEGG terms were also observed. Of note, mitochondrial dysfunction has been hypothesized as a concurrent factor to the pathogenesis of sIBM (Oldfors et al., 2006).

Our second analytical approach integrates the 3 disease groups in a single step, exploiting the fact that, although PCA1 separates control subjects from a joint IBM and/or PM group, PCA2 clearly differentiates sIBM from both PM and controls (Fig. 2C). We ranked genes according to their contribution to PCA2 (measured by the magnitude of the PCA loadings) and selected genes for which the magnitude of the gene-PCA loading was greater than 90% of the maximum gene-PCA loading. GO analysis confirmed enrichment of terms related to RNA metabolism, including RNA splicing, RNA binding, and mRNA metabolic process (Fig. 2D). Reassuringly, the RNA metabolism GO terms found in both our sIBM specific lists, were not enriched in the sublist of 1244 PM specific DEG (Supplementary Table 4).

Of note, sIBM specific DEGs also included *MATR3* and *ZNF9*, known to cause 2 different "RNA-linked" myopathies, distal myopathy type 2 (Senderek et al., 2009), and myotonic dystrophy type 2 (Liquori et al., 2001), respectively.

3.3. Abnormal localization of other hnRNPs in sIBM

HNRNPA2/B1 and *HNRNPH* were significantly downregulated in sIBM (adjusted $p = 0.004$ and adjusted $p = 0.003$, respectively), other hnRNPs including *HNRNPA1* and *HNRNPC* were also downregulated, but without statistical significance after multiple-comparison correction ($p = 0.08$ and $p = 0.03$). Since these genes belong to the same family of ribonucleoproteins as TDP43, and have been shown to interact with TDP43 and to be necessary for its splicing activity

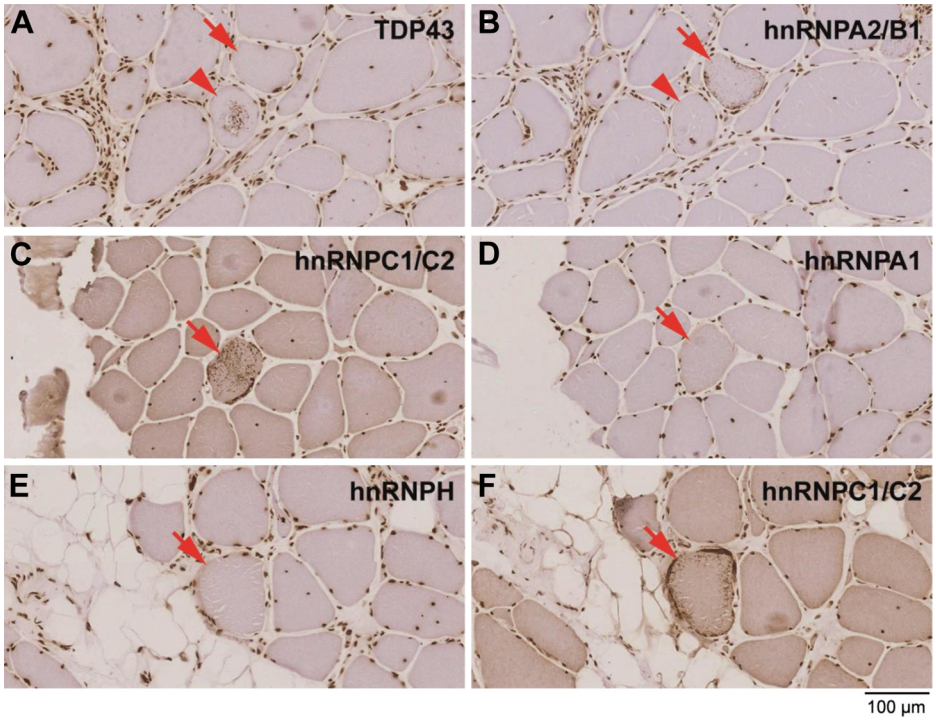

Fig. 3. hnRNPA2/B1 and hnRNPC1/C2 mislocalize in sIBM myofibers. Serial sections of sIBM muscle illustrate the occurrence of cytoplasmic "granular" staining of TDP43 (A), hnRNPA2/B1 (B), and hnRNPC1/C2 (C, F) in different myofibers. hnRNPA1 (D) and hnRNPH (E) do not show mislocalization. Arrows and arrowheads highlight the same fiber on serial sections and illustrate how the abnormal cytoplasmic staining of these proteins can be independent. Abbreviations: hnRNP, heterogenous ribonucleoprotein; sIBM, sporadic inclusion body myositis.

(Buratti et al., 2005; D'Ambrogio et al., 2009), we performed IHC analysis of hnRNPA1, hnRNPA2/B1, hnRNPC1/C2, hnRNPH1, and TDP43, on serial muscle sections. IHC for TDP43 revealed the presence of a cytoplasmic punctate granular staining in nonnecrotic muscle fibers in 5 of 6 IBM patients (Figs. 1 and 3), but none of the PM and control subjects. A similar pattern of diffuse punctate cytoplasmic staining was also present for hnRNPA2/B1 and hnRNPC1/C2 in 4 of 6 and 5 of 6, IBM patients respectively. AMongst sIBM cases, sIBM5 was negative for TDP43, hnRNPA2/B1 and hnRNPC1/C2. These findings were absent in biopsies of control muscle and polymyositis, except for a positive cytoplasmic staining for hnRNPC2 in PM1.

Notably a recent study has identified mutations in *HNRNPA1* and *HNRNPA2/B1* as causative for both ALS and hereditary inclusion body myopathy and described abnormal localization of these proteins, further adding support for the role of their proteins in sIBM (Kim et al., 2013).

Interestingly, the same fiber often showed granular staining for one of these proteins, but not the others (Fig. 2). This is in accordance to the recent finding that hnRNPA1 and hnRNPA2/B1 are not able to induce "cross-seeding" (Kim et al., 2013) and has important pathogenetic implications, suggesting that these proteins do not necessarily cooperate in these stages of disease, but their aggregation may represent alternative, not exclusive, pathways in a common disease process.

3.4. Long intron transcripts in sIBM muscle

Recent work from the Cleveland laboratory has documented an effect of TDP43 loss of function on transcripts containing long introns, and that this effect is common also to another ALS-related hnRNP, FUS (Lagier-Tourenne et al., 2012; Polymenidou et al., 2011a). We therefore investigated if an effect on such transcripts was present in sIBM muscle, and indeed, Gene Set Enrichment Analysis shows that transcripts with introns $>$ 200 Kb are more significantly down-regulated in sIBM (normalized enrichment score 1.65, $p < 0.0001$), although no significant effect is seen in PM versus control subjects (normalized enrichment score 0.67, $p = 0.9$) (Supplementary Fig. 2) (Subramanian et al., 2005). Enrichment and significance are present in the same direction and stronger when the same analysis is performed, as a positive control, on the TDP43 knock-down material used by Polymenidou et al (Polymenidou et al., 2011) (Supplementary Fig. 2).

3.5. MAPT splicing is altered in sIBM

The exon array data also identified exon specific differential expression: using the extended Affymetrix probeset (807,542 probes), and after applying a multiple testing Bonferroni correction (corrected FDR $<$0.05), 157 exonic probes showed differential expression between IBM and control subjects, and 28 between PM and control subjects.

The *MAPT* encoded tau protein has been shown to accumulate and postulated to play a role in sIBM (Mirabella et al., 1996) and *MAPT* alternative splicing plays a role in neurodegenerative diseases (Niblock and Gallo, 2012). Therefore we analyzed *MAPT* splicing and our exon array data showed an increase in exon 6 inclusion in sIBM ($+1.6$ l $\log_2$-fold, FRD adjusted $p < 0.05$) (Fig. 4A). We then validated these findings and also investigated the splicing of *MAPT* exons 2 and 10, known to play a role in neurodegenerative disorders, using RT-PCR and Nanostring probes specific to "spliced-in" and "spliced-out" isoforms. Overall these results indicate the presence of sIBM specific changes in the splicing of *MAPT* exon 6, although changes in exons 2 and 10 are common also to PM samples and possibly reflect inflammatory changes (Fig. 4B–H). Interestingly, exon 6 splicing changes have been previously identified in *postmortem* brain of

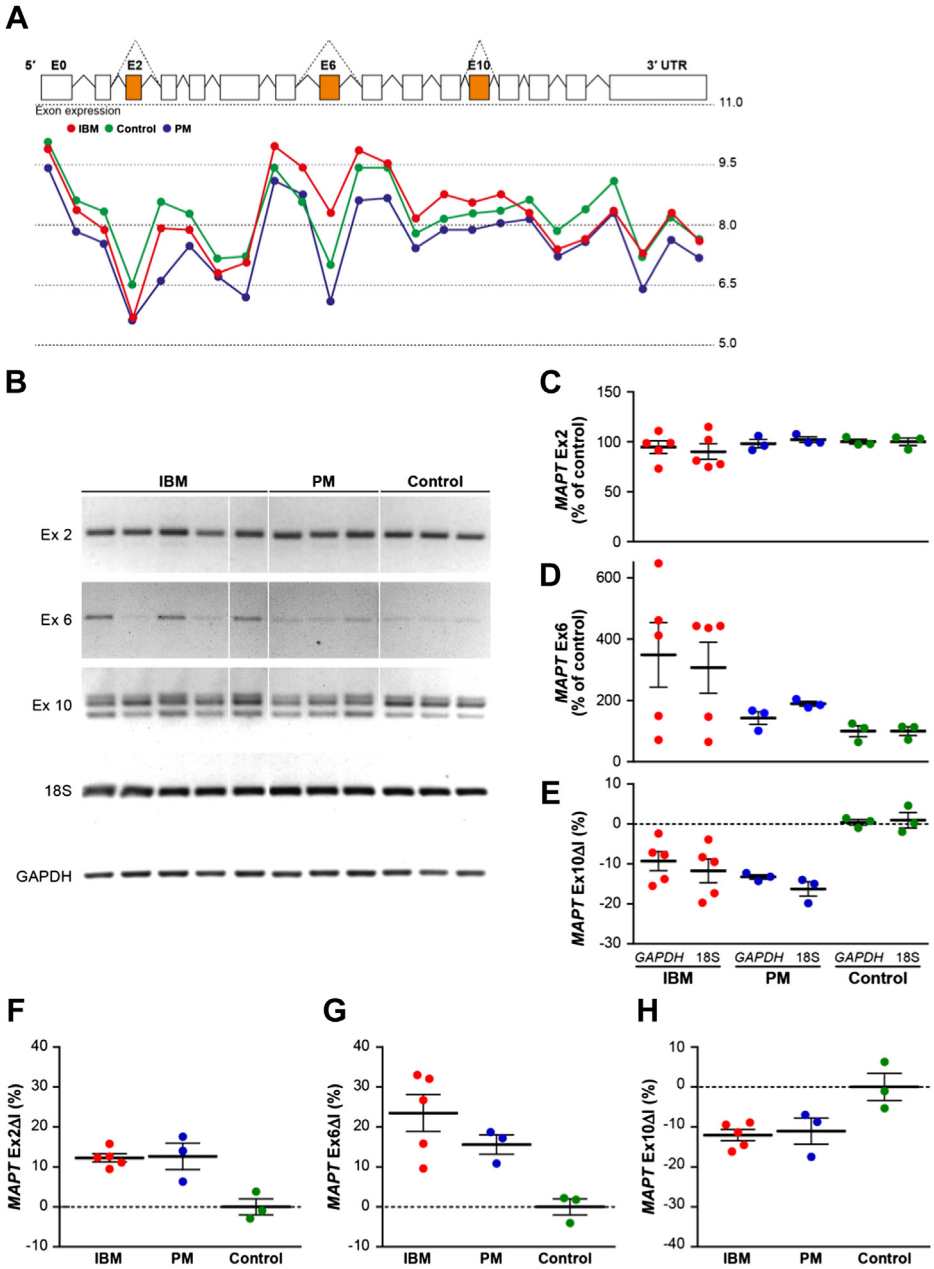

Fig. 4. *MAPT* splicing analysis. (A) Exon arrays show an increased *MAPT* exon 6 inclusion in sIBM (+1.6 l $\log_2$-fold, FRD adjusted $p < 0.05$). (B) Agarose gel electrophoresis of RT-PCR amplicons for *MAPT* exon 2, exon 6, and exon 10 alternative splicing events, and β-actin and *GAPDH* endogenous controls. (C–E) Quantification of RT-PCRs of *MAPT* splicing events normalized to both endogenous controls. (F–H) Nanostring analysis of *MAPT* splicing events. Differential exon inclusion indexes (ΔI) are represented relative to controls. Abbreviation: sIBM, sporadic inclusion body myositis.

myotonic dystrophy type 1 (Leroy et al., 2006), a neurologic disorder in which RNA metabolism plays a clear role.

Conclusions

In conclusion our data reveal widespread changes in RNA metabolism pathways occurring in sIBM TDP43-proteinopathy and are supported by the finding that other novel hnRNPs mislocalize and accumulate in the cytoplasm of sIBM TDP43-proteinopathy (Kim et al., 2013). Importantly, and we believe for the first time in patient tissue, we link a TDP43-proteinopathy with generalized hnRNP misregulation, both transcriptionally and at the level of pathology. These results strongly support the view that RNA metabolism alterations play a role in these disorders, and that downstream RNA misregulation is not the result of TDP43 pathology alone, but is linked to the more complex misregulation of numerous players.

Furthermore, our results highlight similarities between sIBM and ALS and/or FTD and are consistent with mutations in *VCP*, and recently in *HNRNPA1* and *HNRNPA2/B1*, causing both ALS and IBMPFD (Kim et al., 2013). The overlap between sIBM and neurodegenerative disorders, such as ALS and FTD, offers a further tool, through techniques such as single cell capture, for better dissecting and understanding the pathogenesis of these diseases and identifying therapeutic targets.

Disclosure statement

The authors declare no actual of potential conflicts of interest.

Acknowledgements

This work was supported by MRC and MNDA (G1000287/1 Lady Edith Wolfson Fellowship to Pietro Fratta); Medical Research Council, Motor Neurone Disease Association and Thierry Latran Foundation (Elizabeth. M. C. Fisher); The Myositis Support Group (Stephen Brady); Alzheimer's Research UK (Tammaryn Lashley).

The authors thank Ray Young for graphics, Ben White for technical assistance, and UCL Genomics.

Appendix A. Supplementary data

Supplementary data associated with this article can be found, in the online version, at http://dx.doi.org/10.1016/j.neurobiolaging.2013.12.029.

References

Amato, A.A., Barohn, R.J., 2009. Inclusion body myositis: old and new concepts. J. Neurol. Neurosurg. Psychiatr. 80, 1186–1193.

Askanas, V., Engel, W.K., Nogalska, A., 2009. Inclusion body myositis: a degenerative muscle disease associated with intra-muscle fiber multi-protein aggregates, proteasome inhibition, endoplasmic reticulum stress and decreased lysosomal degradation. Brain Pathol. 19, 493–506.

Avendano-Vazquez, S.E., Dhir, A., Bembich, S., Buratti, E., Proudfoot, N., Baralle, F.E., 2012. Autoregulation of TDP-43 mRNA levels involves interplay between transcription, splicing, and alternative polyA site selection. Genes Development 26, 1679–1684.

Benjamini, Y., Hochberg, Y., 1995. Controlling the False Discovery rate: a practical and powerful approach to multiple testing. Journal of the Royal statistical Society. Ser. B (Methodological) 57, 289–300.

Bohan, A., Peter, J., 1975. Polymyositis and dermatomyositis (second of two parts). N. Engl. J. Med. 292, 403–407.

Buratti, E., Brindisi, A., Giombi, M., Tisminetzky, S., Ayala, Y.M., Baralle, F.E., 2005. TDP-43 binds heterogeneous nuclear ribonucleoprotein A/B through its C-terminal tail: an important region for the inhibition of cystic fibrosis transmembrane conductance regulator exon 9 splicing. J. Biol. Chem. 280, 37572–37584.

Cohen, T.J., Lee, V.M.Y., Trojanowski, J.Q., 2011. TDP-43 functions and pathogenic mechanisms implicated in TDP-43 proteinopathies. Trends Mol. Med. 17, 659–667.

D'Agostino, C., Nogalska, A., Engel, W.K., Askanas, V., 2011. In sporadic inclusion body myositis muscle fibres TDP-43-positive inclusions are less frequent and robust than p62 inclusions, and are not associated with paired helical filaments. Neuropathol. Appl. Neurobiol. 37, 315–320.

D'Ambrogio, A., Buratti, E., Stuani, C., Guarnaccia, C., Romano, M., Ayala, Y.M., Baralle, F.E., 2009. Functional mapping of the interaction between TDP-43 and hnRNP A2 in vivo. Nucleic Acids Res. 37, 4116–4126.

Engel, W.K., Askanas, V., 2006. Inclusion-body myositis: clinical, diagnostic, and pathologic aspects. Neurology 66, S20–S29.

Griggs, R.C., Askanas, V., DiMauro, S., Engel, A., Karpati, G., Mendell, J.R., Rowland, L.P., 1995. Inclusion body myositis and myopathies. Ann. Neurol. 38, 705–713.

Hernandez Lain, A., Millecamps, S., Dubourg, O., Salachas, F., Bruneteau, G., Lacomblez, L., LeGuern, E., Seilhean, D., Duyckaerts, C., Meininger, V., Mallet, J., Pradat, P.-F., 2011. Abnormal TDP-43 and FUS proteins in muscles of sporadic IBM: similarities in a TARDBP-linked ALS patient. J. Neurol. Neurosurg. Psychiatr. 82, 1414–1416.

Huang, D.W., Sherman, B.T., Lempicki, R.A., 2009. Systematic and integrative analysis of large gene lists using DAVID bioinformatics resources. Nat. Protoc. 4, 44–57.

Irizarry, R.A., Bolstad, B.M., Collin, F., Cope, L.M., Hobbs, B., Speed, T.P., 2003. Summaries of Affymetrix GeneChip probe level data. Nucleic Acids Res. 31, e15.

Johnson, J.O., Mandrioli, J., Benatar, M., Abramzon, Y., Van Deerlin, V.M., Trojanowski, J.Q., Gibbs, J.R., Brunetti, M., Gronka, S., Wuu, J., Ding, J., McCluskey, L., Martinez-Lage, M., Falcone, D., Hernandez, D.G., Arepalli, S., Chong, S., Schymick, J.C., Rothstein, J., Landi, F., Wang, Y.-D., Calvo, A., Mora, G., Sabatelli, M., Monsurrò, M.R., Battistini, S., Salvi, F., Spataro, R., Sola, P., Borghero, G., Galassi, G., Scholz, S.W., Taylor, J.P., Restagno, G., Chiò, A., Traynor, B.J., 2010. Exome sequencing reveals VCP mutations as a cause of familial ALS. Neuron 68, 857–864.

Kabashi, E., Valdmanis, P.N., Dion, P., Spiegelman, D., McConkey, B.J., Vande Velde, C., Bouchard, J.-P., Lacomblez, L., Pochigaeva, K., Salachas, F., Pradat, P.-F., Camu, W., Meininger, V., Dupre, N., Rouleau, G.A., 2008. TARDBP mutations in individuals with sporadic and familial amyotrophic lateral sclerosis. Nat. Genet. 40, 572–574.

Kawahara, Y., Mieda-Sato, A., 2012. TDP-43 promotes microRNA biogenesis as a component of the Drosha and Dicer complexes. Proc. Natl. Acad. Sci. U.S.A 109, 3347–3352.

Kim, H.J., Kim, N.C., Wang, Y.-D., Scarborough, E.A., Moore, J., Diaz, Z., MacLea, K.S., Freibaum, B., Li, S., Molliex, A., Kanagaraj, A.P., Carter, R., Boylan, K.B., Wojtas, A.M., Rademakers, R., Pinkus, J.L., Greenberg, S.A., Trojanowski, J.Q., Traynor, B.J., Smith, B.N., Topp, S., Gkazi, A.-S., Miller, J., Shaw, C.E., Kottlors, M., Kirschner, J., Pestronk, A., Li, Y.R., Ford, A.F., Gitler, A.D., Benatar, M., King, O.D., Kimonis, V.E., Ross, E.D., Weihl, C.C., Shorter, J., Taylor, J.P., 2013. Mutations in prion-like domains in hnRNPA2B1 and hnRNPA1 cause multisystem proteinopathy and ALS. Nature 495, 467–473.

Küsters, B., van Hoeve, B.J.A., Schelhaas, H.J., Ter Laak, H., van Engelen, B.G.M., Lammens, M., 2009. TDP-43 accumulation is common in myopathies with rimmed vacuoles. Acta Neuropathol. 117, 209–211.

Lagier-Tourenne, C., Polymenidou, M., Hutt, K.R., Vu, A.Q., Baughn, M., Huelga, S.C., Clutario, K.M., Ling, S.-C., Liang, T.Y., Mazur, C., Wancewicz, E., Kim, A.S., Watt, A., Freier, S., Hicks, G.G., Donohue, J.P., Shiue, L., Bennett, C.F., Ravits, J., Cleveland, D.W., Yeo, G.W., 2012. Divergent roles of ALS-linked proteins FUS/TLS and TDP-43 intersect in processing long pre-mRNAs. Nat. Neurosci. 15, 1488–1497.

Lee, E.B., Lee, V.M.-Y., Trojanowski, J.Q., 2012. Gains or losses: molecular mechanisms of TDP43-mediated neurodegeneration. Nat. Rev. Neurosci. 13, 38–50.

Leroy, O., Wang, J., Maurage, C.-A., Parent, M., Cooper, T., Buée, L., Sergeant, N., Andreadis, A., Caillet-Boudin, M.-L., 2006. Brain-specific change in alternative splicing of Tau exon 6 in myotonic dystrophy type 1. Biochim. Biophys. Acta 1762, 460–467.

Liquori, C.L., Ricker, K., Moseley, M.L., Jacobsen, J.F., Kress, W., Naylor, S.L., Day, J.W., Ranum, L.P., 2001. Myotonic dystrophy type 2 caused by a CCTG expansion in intron 1 of ZNF9. Science 293, 864–867.

Mackenzie, I.R., Rademakers, R., Neumann, M., 2010. TDP-43 and FUS in amyotrophic lateral sclerosis and frontotemporal dementia. Lancet Neurol. 9, 995–1007.

Mirabella, M., Alvarez, R.B., Bilak, M., Engel, W.K., Askanas, V., 1996. Difference in expression of phosphorylated tau epitopes between sporadic inclusion-body myositis and hereditary inclusion-body myopathies. J. Neuropathol. Exp. Neurol. 55, 774–786.

Mishra, M., Paunesku, T., Woloschak, G.E., Siddique, T., Zhu, L.J., Lin, S., Greco, K., Bigio, E.H., 2007. Gene expression analysis of frontotemporal lobar degeneration of the motor neuron disease type with ubiquitinated inclusions. Acta Neuropathol. 114, 81–94.

Nalbandian, A., Donkervoort, S., Dec, E., Badadani, M., Katheria, V., Rana, P., Nguyen, C., Mukherjee, J., Caiozzo, V., Martin, B., Watts, G.D., Vesa, J., Smith, C., Kimonis, V.E., 2011. The multiple faces of valosin-containing protein-associated diseases: inclusion body myopathy with Paget's disease of bone, frontotemporal dementia, and amyotrophic lateral sclerosis. J. Mol. Neurosci. 45, 522–531.

Needham, M., Mastaglia, F.L., 2007. Inclusion body myositis: current pathogenetic concepts and diagnostic and therapeutic approaches. Lancet Neurol. 6, 620–631.

Niblock, M., Gallo, J.-M., 2012. Tau alternative splicing in familial and sporadic tauopathies. Biochem. Soc. Trans. 40, 677–680.

Oldfors, A., Moslemi, A.R., Jonasson, L., Ohlsson, M., Kollberg, G., Lindberg, C., 2006. Mitochondrial abnormalities in inclusion-body myositis. Neurology 66, S49–S55.

Oliνι, M., Januι, A., Moreno, D., Gαmez, J., Torrejσn-Escribano, B., Ferrer, I., 2009. TAR DNA-Binding protein 43 accumulation in protein aggregate myopathies. J. Neuropathol. Exp. Neurol. 68, 262–273.

Polymenidou, M., Lagier-Tourenne, C., Hutt, K.R., Huelga, S.C., Moran, J., Liang, T.Y., Ling, S.-C., Sun, E., Wancewicz, E., Mazur, C., Kordasiewicz, H., Sedaghat, Y., Donohue, J.P., Shiue, L., Bennett, C.F., Yeo, G.W., Cleveland, D.W., 2011a. Long pre-mRNA depletion and RNA missplicing contribute to neuronal vulnerability from loss of TDP-43. Nat. Neurosci. 14, 459–468.

Rayavarapu, S., Coley, W., Nagaraju, K., 2011. An update on pathogenic mechanisms of inflammatory myopathies. Curr. Opin. Rheumatol. 23, 579–584.

Salajegheh, M., Pinkus, J.L., Taylor, J.P., Amato, A.A., Nazareno, R., Baloh, R.H., Greenberg, S.A., 2009. Sarcoplasmic redistribution of nuclear TDP-43 in inclusion body myositis. Muscle Nerve 40, 19–31.

Senderek, J., Garvey, S.M., Krieger, M., Guergueltcheva, V., Urtizberea, A., Roos, A., Elbracht, M., Stendel, C., Tournev, I., Mihailova, V., Feit, H., Tramonte, J., Hedera, P., Crooks, K., Bergmann, C., Rudnik-Schφneborn, S., Zerres, K., Lochmόller, H., Seboun, E., Weis, J., Beckmann, J.S., Hauser, M.A., Jackson, C.E., 2009. Autosomal-dominant distal myopathy associated with a recurrent missense mutation in the gene encoding the nuclear matrix protein, matrin 3. Am. J. Hum. Genet. 84, 511–518.

Smyth, G.K., 2004. Linear models and empirical bayes methods for assessing differential expression in microarray experiments. Stat. Appl. Genet. Mol. Biol. 3. Article3.

Sreedharan, J., Blair, I.P., Tripathi, V.B., Hu, X., Vance, C., Rogelj, B., Ackerley, S., Durnall, J.C., Williams, K.L., Buratti, E., Baralle, F., de Belleroche, J., Mitchell, J.D., Leigh, P.N., Al-Chalabi, A., Miller, C.C., Nicholson, G., Shaw, C.E., 2008. TDP-43 mutations in familial and sporadic amyotrophic lateral sclerosis. Science 319, 1668–1672.

Subramanian, A., Tamayo, P., Mootha, V.K., Mukherjee, S., Ebert, B.L., Gillette, M.A., Paulovich, A., Pomeroy, S.L., Golub, T.R., Lander, E.S., Mesirov, J.P., 2005. Gene set enrichment analysis: a knowledge-based approach for interpreting genome-wide expression profiles. PNAS 102, 15545–15550.

Tollervey, J.R., Curk, T., Rogelj, B., Briese, M., Cereda, M., Kayikci, M., Kφnig, J., Hortobαgyi, T., Nishimura, A.L., Zupunski, V., Patani, R., Chandran, S., Rot, G., Zupan, B., Shaw, C.E., Ule, J., 2011a. Characterizing the RNA targets and position-dependent splicing regulation by TDP-43. Nat. Neurosci. 14, 452–458.

Weihl, C.C., Temiz, P., Miller, S.E., Watts, G., Smith, C., Forman, M., Hanson, P.I., Kimonis, V., Pestronk, A., 2008. TDP-43 accumulation in inclusion body myopathy muscle suggests a common pathogenic mechanism with frontotemporal dementia. J. Neurol. Neurosurg. Psychiatr. 79, 1186–1189.